Hindawi
Geofluids
Volume 2022, Article ID 6768370, 8 pages
https://doi.org/10.1155/2022/6768370

Research Article

Evolution Mechanism of Mesocrack and Macrocrack Propagation in Carbonaceous Mudstone under the Action of Dry-Wet Cycles

S. N. Li,[1] **Z. H. Huang**,[2] **Q. Liang**,[1] **J. Liu**,[1] **S. L. Luo**,[3] **and W. Q. Zhou**[1]

[1]*School of Architectural Engineering, Hunan Institute of Engineering, Xiangtan Hunan 411104, China*
[2]*School of Mechanical Engineering, Hunan Institute of Engineering, Xiangtan Hunan 411104, China*
[3]*College of Civil Engineering, Changsha University, Changsha 410022, China*

Correspondence should be addressed to S. N. Li; 2561720910@qq.com

Received 23 February 2022; Revised 26 April 2022; Accepted 3 May 2022; Published 19 July 2022

Academic Editor: Yi Liu

The crack propagation evolution of carbonaceous mudstone under the action of dry-wet cycles is an important cause of the unstable failure of this type of slope. This paper attempts to reveal the evolution mechanism of mesocrack and macrocrack propagation in carbonaceous mudstone under the action of dry-wet cycles from chemical, physical, and mechanical perspectives. Firstly, the soaking solution of carbonaceous mudstone during the dry-wet cycles was extracted for an ion concentration test to analyze the chemical reactions of carbonaceous mudstone. Then, CT scans were performed on the carbonaceous mudstone samples to study the changing pattern of mesostructure of carbonaceous mudstone during the dry-wet cycles. In the end, the mechanical properties and failure characteristics of carbonaceous mudstone after dry-wet cycles were studied by triaxial compression tests. The results showed that chemical reactions such as calcite dissolution, potassium feldspar hydrolysis, and sodium feldspar hydrolysis occurred during the dry-wet cycle of carbonaceous mudstone. Affected by the dry-wet cycles, the mesostructure of the carbonaceous mudstone gradually changed from face-face contact and edge-face contact to edge-corner contact and corner-corner contact, and the interlayer flake structure was opened and was locally curled and fractured. With the increase in the number of dry-wet cycles, the failure characteristic of carbonaceous mudstone transformed from tensile failure to shear failure, the failure surface of carbonaceous mudstone was deflected from 90° to 60°, and the crack propagation path of carbonaceous mudstone became more complicated. The chemical reaction of carbonaceous mudstone minerals during the dry-wet cycle is an important reason for the initiation and development of pores. The dry-wet cycle aggregates the propagation of mesocracks and structural disorder, transforming the uniform stress state of the rock mesostructure to the concentrated stress state, which is the important reason for the macrocrack propagation evolution of carbonaceous mudstone.

1. Introduction

Carbonaceous mudstones are widely distributed in Permian and Devonian strata in southwest China [1, 2]. They are rich in clay minerals and primary fissures and have properties such as easy softening and disintegration after water absorption [3]. Due to the hot and humid climate in southwest China, excavated carbonaceous mudstone cutting slopes are subjected to dry-wet cycles, leading to the initiation of a large number of cracks in slopes. Once the slope cracks are connected to each other, the slope instability failure occurs immediately [4, 5]. Therefore, studying the mechanism of crack propagation evolution of carbonaceous mudstone under the action of dry-wet cycles is significant for the prevention and control of this kind of slope disaster.

The crack propagation evolution of soft rocks under dry-wet cycles has been a hot research topic [6–8]. Soft rock crack initiation, propagation, and coalescence are complex

physical, chemical, and mechanical water-rock interaction processes [9–12], which are closely related to mineral composition, mesostructure, and stress state [13–15]. Mineral dissolution and water absorption swelling are important causes of crack initiation and propagation of soft rock [16–18]. In addition, the primary joints and fissures provide a convenient channel for the water-rock reaction, which promotes crack propagation and coalescence [19–21]. Due to various geological tectonic effects, the minerals, joints, and fissures in soft rocks are distributed disorderly, complicating the evolution of crack propagation of soft rock [22]. Jiang et al. [23] concluded that the water absorption swelling of soft rocks is anisotropic with the swelling deformation being more significant in the vertical bedding direction, and therefore, cracks are more likely to propagate in the parallel layered direction. Zhao et al. [24] found that the cracks initiate and propagate from the developed part of the cementitious material after soft rocks were soaked in water. Zhang et al. [25] found that the mineral composition and mesostructure of carbonaceous mudstone are altered under the action of dry-wet cycles. Liu et al. and Coombes and Naylor [26–28] suggested that affected by dry-wet cycles, the pores of soft rocks gradually converge and connect, and the neat and dense microstructure of soft rocks becomes disordered and loose. Pineda et al. [29] regarded that the development and propagation of cracks on the joint surface under the action of dry-wet cycles are an important cause of the deterioration of the mechanical properties of rocks. Hua et al. and Li et al. [30, 31] found that dry-wet cycles have significant effects on the evolution of rock crack propagation and failure mode, and the crack failure surface changed after several dry-wet cycles.

In summary, previous studies have only briefly analyzed the laws of mesocrack or macrocrack propagation in the process of water-rock interaction. However, the chemical, physical, and mechanical mechanisms of macrocrack and mesocrack propagation evolution in carbonaceous mudstone under the action of dry-wet cycles have rarely been investigated. In this paper, the chemical composition, mesostructure, and mechanical properties of carbonaceous mudstone under the action of dry-wet cycles are studied to reveal the intrinsic mechanism of macrocrack and mesocrack propagation evolution of carbonaceous mudstone under dry-wet cycles. The research results will provide a reference for the prevention and control of disasters in carbonaceous mudstone cutting slopes.

2. Sample Characteristics and Test Process

2.1. Sample Characteristics. The samples of carbonaceous mudstone were taken from the high slope (70.0-80.0 m) of the Liuzhai-Hechi Expressway in Guangxi province. The samples were dark gray and medium weathered, with uniform grains and microfracture development. The diffraction pattern of carbonaceous mudstone obtained by the X-ray diffraction experiment is shown in Figure 1. The phase analysis results of carbonaceous mudstone are shown in Table 1. The carbonaceous mudstone block mass was made into 50 mm × 100 mm samples by the anhydrous drilling method.

2.2. Test Process. The test process is shown in Figure 2. Firstly, the samples were subjected to dry-wet cycles. Secondly, the soaking solution of carbonaceous mudstone during dry-wet cycles was taken with a liquid-holding bottle for the inductively coupled plasma mass spectrometry (ICP-MS) test. Then, randomly selected samples were sliced, and the mesostructure of carbonaceous mudstone was scanned by an electron microscope. In the end, triaxial compression tests were performed on the carbonaceous mudstone samples to analyze the macrocrack propagation law of the samples subjected to dry-wet cycles.

2.2.1. Dry-Wet Cycle Experiment. In order to simulate the extreme climate conditions in Guangxi province, the samples were dried in an oven at 60°C for 24 h and cooled to room temperature in the moisturizing cylinder, and then naturally saturated with water for 24 h. Each dry-wet cycle lasted for 48 h. The carbonaceous mudstone samples were subjected to 0, 5, 10, and 15 dry-wet cycles, respectively.

2.2.2. Inductively Coupled Plasma Mass Spectroscopy Test. The aqueous solutions soaking the carbonaceous mudstone samples were collected and stored in sealed liquid-holding bottles. The iCAP RQ ICP-MS was applied to test the cation concentration in the aqueous solution after wet-dry cycles. The tested cations were the metal cations of the main minerals of the carbonaceous mudstone.

2.2.3. Scanning Electron Microscopy Observation. After dry-wet cycles, randomly selected samples were made into a size of about 5 × 10 × 10 mm with a fine steel wire saw, and the dust on the sample surface was cleaned using ear wash balls. The gold spray was performed for the cleaned samples, and then, the mesostructure of the samples was scanned by an S-3000N scanning electron microscope.

2.2.4. Triaxial Compression Test. The MTS material testing system was used for the triaxial compression test of carbonaceous mudstone. The confining pressure was set to 2 MPa to simulate the real stress environment of the rocks of the carbonaceous mudstone cutting slope. The confining pressure was firstly applied at a rate of 0.05 MPa/s, and after 2 min, the axial load was applied at a rate of 0.5-1.0 MPa/s.

3. Test Result Analysis

3.1. Analysis of Chemical Reactions of Minerals. The concentration of metal cations in aqueous solutions under the action of dry-wet cycles is shown in Table 2. It can be seen that the concentration of metal cations increases with the number of dry-wet cycles, and in terms of the concentration increase, the metal cations are ranked as $Ca^{2+} > K^{+} > Na^{+} > Fe^{2+} > Al^{3+}$. The concentration of Ca^{2+} was one order of magnitude higher than that of K^{+}, Na^{+}, and Fe^{2+} and two orders of magnitude higher than that of Al^{3+}.

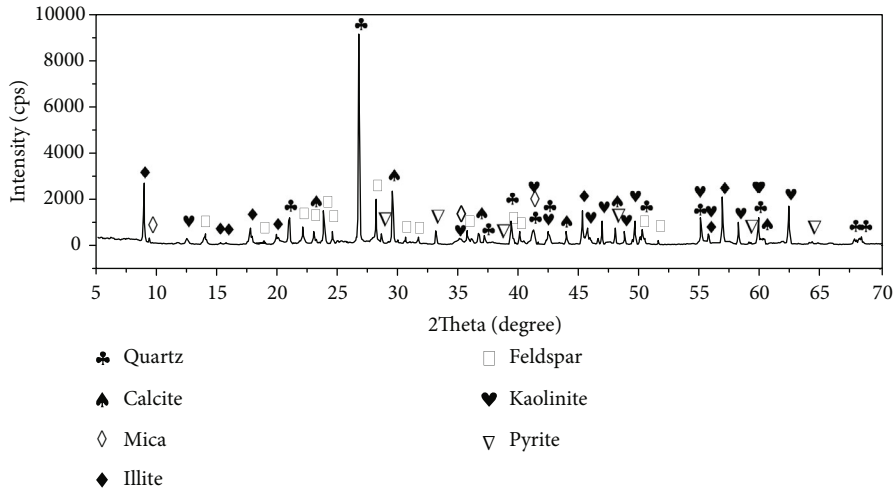

Figure 1: Diffraction pattern of carbonaceous mudstone.

Table 1: The mineral component of carbonaceous mudstone.

Mineral composition	Illite	Kaolinite	Quartz	Feldspar	Calcite	Pyrite	Mica
Content (%)	18.8	21.4	41.5	5.8	7.6	2.1	2.8

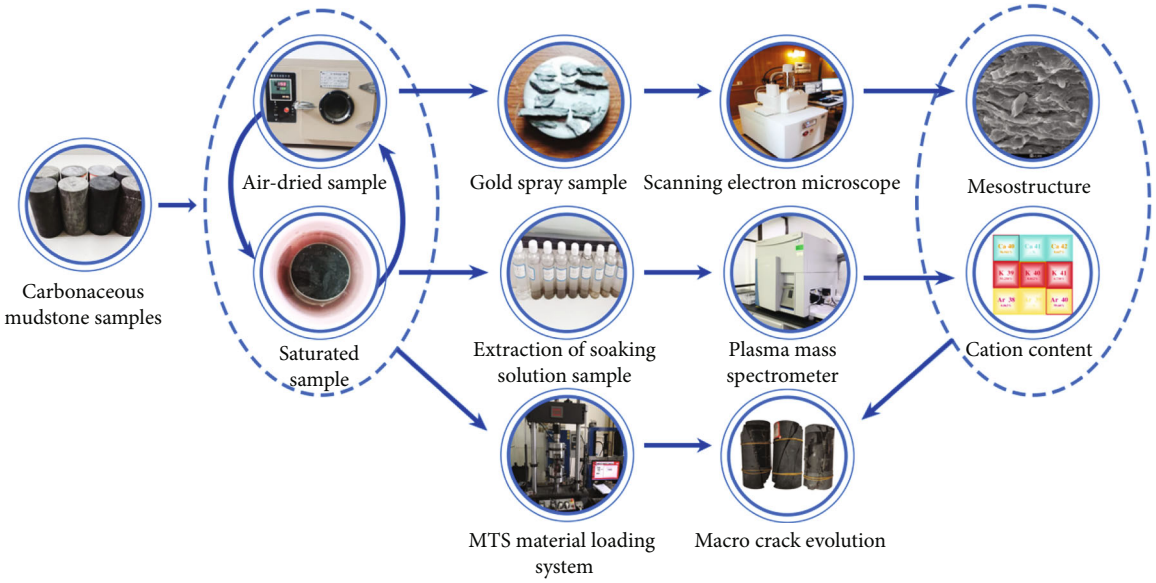

Figure 2: Test process.

Table 2: Concentration of metal cations in aqueous solution under dry-wet cycles.

Concentration of metal cations ($mg \cdot L^{-1}$)	Number of dry-wet cycles 0	5	10	15
Ca^{2+}	5.20	188.65	367.62	528.58
K^{+}	1.80	6.88	13.71	19.65
Na^{+}	1.40	9.10	11.77	14.60
Al^{3+}	0.30	0.88	1.06	1.22
Fe^{2+}	5.50	6.34	9.87	11.38

Based on the electroneutrality principle, it can be assumed that the following chemical reactions occur in the carbonaceous mudstone during the dry-wet cycles.

(1) Calcite dissolution

$$CaCO_3 + CO_2 + H_2O = Ca^{2+} + 2HCO_3^- \quad (1)$$

After the calcite reacts with carbon dioxide and water, calcite dissolves, and calcium ions precipitate, resulting in a

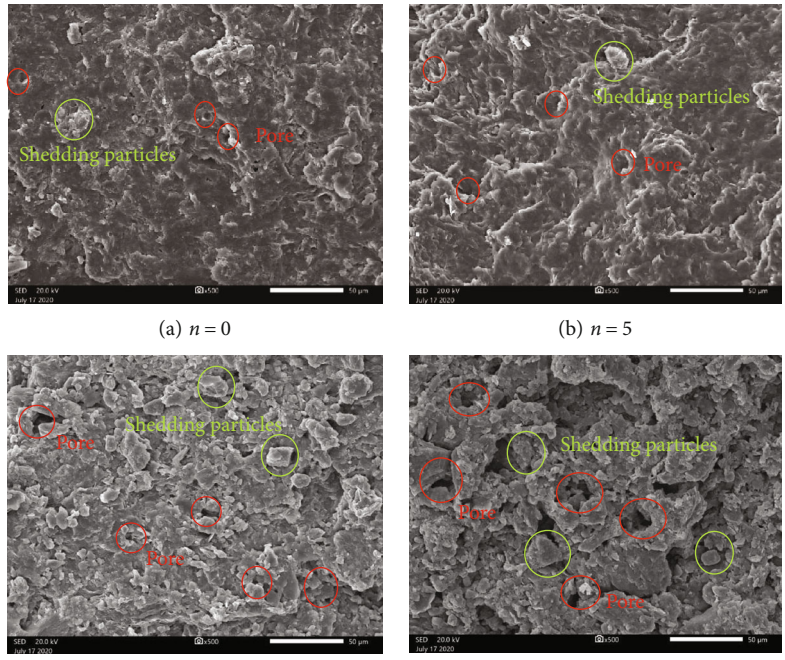

(a) $n = 0$ (b) $n = 5$

(c) $n = 10$ (d) $n = 15$

Figure 3: Scanning electron microscopy observation for carbonaceous mudstone in parallel layered direction.

decrease in calcite content and an increase in Ca^{2+} mass concentration in the aqueous solution.

(2) Feldspar (potassium feldspar, sodium feldspar) hydrolysis

$$KAlSi_3O_8 + 5.5H_2O = 0.5Al_2Si_3O_5(OH)_4 + K^+ + OH^- + 2H_4SiO_4 \quad (2)$$

$$NaAlSi_3O_8 + 5.5H_2O = 0.5Al_2Si_3O_5(OH)_4 + Na^+ + OH^- + 2H_4SiO_4 \quad (3)$$

After the hydrolysis of potassium feldspar and sodium feldspar, kaolinite is formed and Na^+ and K^+ precipitate, which causes the decrease of feldspar content and increase of kaolinite content in carbonaceous mudstone and the increase of Na^+ and K^+ mass concentration in aqueous solution.

(3) Pyrite hydrolysis

$$FeS_2 + 3.5O_2 + H_2O = Fe^{2+} + 2SO_4^{2-} + 2H^+ \quad (4)$$

After the oxidation reaction between oxygen dissolved in water and pyrite, Fe^{2+} precipitates out, increasing the concentration of Fe^{2+} in the water solution. The oxidation products adsorbed on the surface of pyrite will passivate and inhibit the oxidation reaction, resulting in the weakening of the oxidation reaction intensity of pyrite, which is the reason for the content of pyrite and the mass concentration of Fe^{2+} changing insignificantly.

3.2. Microstructure Change Pattern. The results of scanning electron microscopy observation for the carbonaceous mudstone in the parallel layered direction are shown in Figure 3. Before the dry-wet cycle, as shown in Figure 3(a), the carbonaceous mudstone sample has a dense structure, a flat surface, and a mesostructure of face-face contact, and the pores are scattered disorderly among the particles. After 5 dry-wet cycles, as shown in Figure 3(b), there are some shedding particles. The number of pores increases, and the surface becomes rough and bumpy. The skeleton structure with the face-face and edge-face contact is gradually distorted. After 10 dry-wet cycles, as shown in Figure 3(c), more particles are exposed, and the outline is clear. The number of shedding particles increases significantly, and the number and size of pores increase. The particle structure changes from face-face contact and edge-face contact to edge-edge contact and edge-corner contact and becomes loose. After 15 dry-wet cycles, as shown in Figure 3(d), there are a large number of shedding particles. Many dissolution pits appear on the sample surface. The particles are corroded, and the outline becomes blurred and rough. The mesostructure changes from edge-edge contact and edge-corner contact to edge-corner contact and corner-corner contact.

The results for scanning electron microscopy observation of the carbonaceous mudstone in the vertical layered direction are shown in Figure 4. Before the dry-wet cycle, as shown in Figure 4(a), the carbonaceous mudstone has a stacked flake structure, and flake frameworks are arranged regularly and cemented by clay minerals. There are a small number of shedding particles among the layers, where the pores are scattered disorderly. After 5 dry-wet cycles, as shown in Figure 4(b), there are a large number of shedding

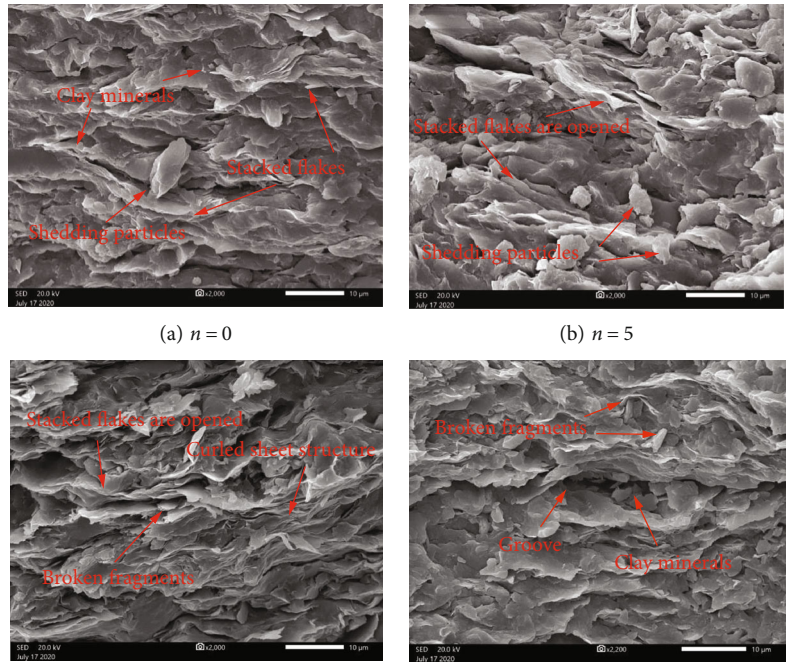

(a) $n = 0$ (b) $n = 5$

(c) $n = 10$ (d) $n = 15$

Figure 4: Scanning electron microscopy observation for carbonaceous mudstone in the vertical layered direction.

particles. The flake framework is gradually opened and begins to curl, which causes the interlayer roughness to increase. After 10 dry-wet cycles, as shown in Figure 4(c), the flake structures are more seriously curled and disordered; the opening spacing between layers is significantly increased. There are some fractures and fragments in local flake structures. The number of pores increases dramatically, and they present a coalescence trend. After 15 dry-wet cycles, as shown in Figure 4(d), the clay minerals are basically dissolved. A large number of flake structures are fractured, and some fragments fall off. Some interlayer grooves are formed on the surface of the flake structure, and the clay minerals buried deep in the flake structure are exposed.

3.3. Analysis of Mechanical Properties. The stress-strain curves of the carbonaceous mudstone are shown in Figure 5. It can be seen that with the increase in the number of dry-wet cycles, the stress-strain curve becomes more gentle, the nonlinearity of the compression stage and crack propagation stage is enhanced, the slope of the linear elastic stage and peak stress gradually decrease, and the strain at peak stress increases. The stress decreases more slowly after rock failure, and the failure mode of the rock changes from brittle failure to ductile failure.

The failure characteristics of the carbonaceous mudstone samples are shown in Figure 6. It can be seen that before the dry-wet cycle, as shown in Figure 6(a), the damaged sample shows 3 vertical cracks through the sample with a small amount of debris dislodged and presents tensile failure characteristics. After 5 dry-wet cycles, as shown in Figure 6(b), a vertical crack of about 90° appears on the carbonaceous mudstone, and a branch crack occurs at the upper middle

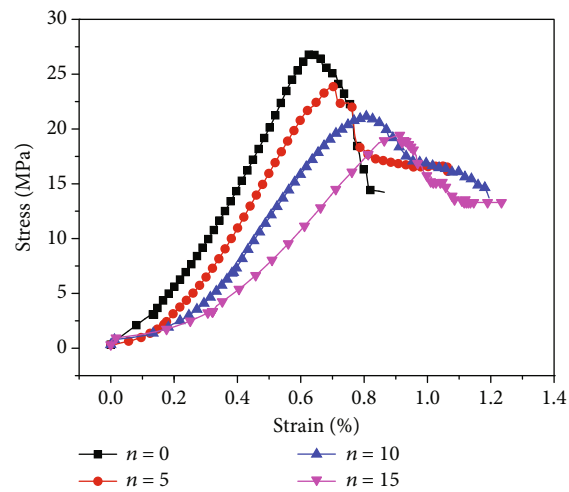

Figure 5: Stress-strain curve of carbonaceous mudstone.

of the sample (about 1/3 of the sample height) and extends to the top. The sample presents tension-shear failure characteristics. A large number of fragments are shed from the failure surface of the sample. After 10 dry-wet cycles, as shown in Figure 6(c), the cracks extending through the sample show a deflection of about 60°, which indicates typical shear failure. There are many fragments shed from the top and low surfaces of the sample. After 15 dry-wet cycles, as shown in Figure 6(d), two oblique cracks of about 60° appear on the damaged sample. One crack extends through the sample, with local branch cracks presenting disordered propagation. The other crack extends from the middle of the bottom to 2/3 of the height of the sample. There are fragments shedding

(a) $n = 0$ (b) $n = 5$ (c) $n = 10$ (d) $n = 15$

Figure 6: Failure characteristics of carbonaceous mudstone sample.

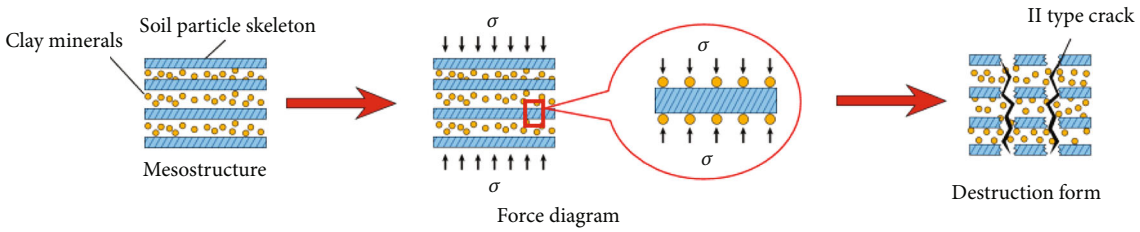

(a) Mesostructure of carbonaceous mudstone without dry-wet cycle

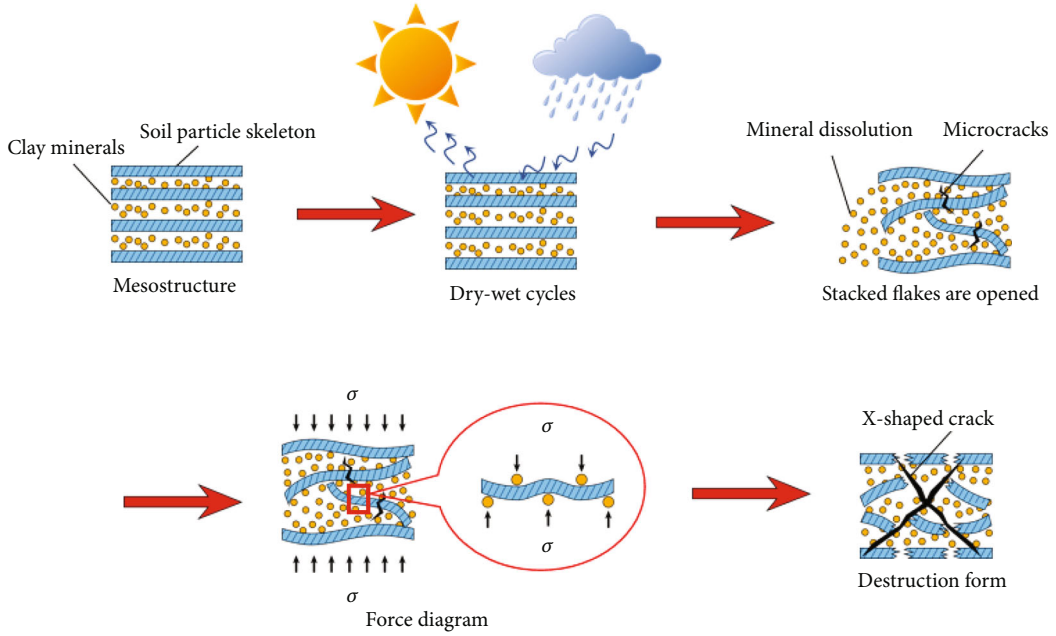

(b) Mesostructure of carbonaceous mudstone after dry-wet cycle

Figure 7: Mesostructure of carbonaceous mudstone.

from some parts of the failure surface. In summary, it can be concluded that the dry-wet cycle will deflect macrocrack propagation of the carbonaceous mudstone sample, and the failure mode of the sample changes from tensile failure to shear failure, while the ductile failure characteristics are enhanced.

4. Evolution Mechanism of Carbonaceous Mudstone Crack Propagation

According to electron microscope scanning, the mesostructure of carbonaceous mudstone can be simplified to a stacked flake structure composed of cementing minerals

and skeletons, as shown in Figure 7(a). The mesostructure of carbonaceous mudstone before the dry-wet cycle is neat and dense, and the stacked flakes are uniformly stressed after being loaded. As the interlayer stress increases, the mesostructure of carbonaceous mudstone undergoes tensile failure along the direction of the maximum shear stress. The crack propagation path is regular owing to the organized and neat mesostructure. The mesostructure of carbonaceous mudstone under the action of dry-wet cycles is shown in Figure 7(b). The soluble minerals between the layers of the stacked flake structure of carbonaceous mudstone are gradually dissolved, which causes the pores in the mesostructure to gradually propagate and connect. In addition, the skeleton of the stacked flake structure is extruded and deformed due to the swelling of minerals after water absorption and volume expansion during the mineral reaction, and the skeleton structure is gradually transformed from face-face contact and edge-face contact to edge-corner contact and corner-corner contact. The flake skeleton of the mesostructure is locally curled and fractured. With the mesostructure under stress, stress concentrations are easy to occur at the edge-corner and corner-corner contact points of the skeleton. The shear failure occurs after the flake skeleton is stressed, and the cracks propagate along the weak parts of the mesostructure. Due to the effect of dry-wet cycles, the mesostructure of carbonaceous mudstone is disordered and the mesostructure is not uniformly stressed. It is an important reason for the chaotic crack propagation path.

5. Conclusion

In this paper, the mechanism of macrocrack and mesocrack propagation evolution in carbonaceous mudstone under the action of dry-wet cycles is studied through a series of experiments, and the following conclusions can be drawn.

(1) Calcite dissolution, potassium feldspar hydrolysis, and sodium feldspar hydrolysis are the important reasons for the initiation and development of cracks in carbonaceous mudstone during dry-wet cycles

(2) With the increase in the number of dry-wet cycles, the mesostructure of carbonaceous mudstone gradually changes from face-face contact and edge-face contact to edge-corner contact and corner-corner contact, and the interlayer flake structures are opened and are more seriously curled and fractured

(3) Under the influence of dry-wet cycles, the bearing capacity of carbonaceous mudstone is reduced. The failure mode of rock changes from tensile failure to shear failure, the failure surface is deflected from 90° to 60°, and the crack propagation path becomes complicated

(4) Water absorption swelling and chemical reaction of mineral of carbonaceous mudstone under the action of dry-wet cycles lead to the changes in the stress form of the mesostructure, which directly transforms the macrocrack propagation mode during the damage of carbonaceous mudstone under load. These findings reveal the mechanism of macrocrack and mesocrack propagation evolution in carbonaceous mudstone under the action of dry-wet cycles

Data Availability

The data used to support the findings of this study are available from the corresponding author upon request.

Conflicts of Interest

The authors declare that they have no conflicts of interest.

Acknowledgments

This research was funded by the National Natural Science Foundation of China (52108405), Natural Science Foundation of Hunan Province Project (2022JJ40122), and Scientific Research Foundation of Hunan Provincial Education Department (20A118, 21A0462, and 21B0659).

References

[1] L. Zeng, H. Yu, Q. Gao, and H. B. Bian, "Mechanical behavior and microstructural mechanism of improved disintegrated carbonaceous mudstone," *Journal of Central South University*, vol. 27, no. 7, pp. 1992–2002, 2020.

[2] L. Zeng, H. C. Yu, J. Liu, Q. F. Gao, and H. B. Bian, "Mechanical behaviour of disintegrated carbonaceous mudstone under stress and cyclic drying/wetting," *Construction and Building Materials*, vol. 282, article 122656, 2021.

[3] L. Zeng, J. T. Luo, J. Liu, Q. F. Gao, and H. B. Bian, "Disintegration characteristics and mechanisms of carbonaceous mudstone subjected to load and cyclic drying–wetting," *Journal of Materials in Civil Engineering*, vol. 33, no. 8, article 04021195, 2021.

[4] Q. F. Gao, D. Zhao, L. Zeng, and H. Dong, "A pore size distribution-based microscopic model for evaluating the permeability of clay," *KSCE Journal of Civil Engineering*, vol. 23, no. 12, pp. 5002–5011, 2019.

[5] L. Zeng, L. Y. Xiao, J. H. Zhang, and Q. F. Gao, "Effect of the characteristics of surface cracks on the transient saturated zones in colluvial soil slopes during rainfall," *Bulletin of Engineering Geology and the Environment*, vol. 79, no. 2, pp. 699–709, 2020.

[6] M. L. Lin, F. S. Jeng, L. S. Tsai, and T. H. Huang, "Wetting weakening of tertiary sandstones—microscopic mechanism," *Environmental Geology*, vol. 48, no. 2, pp. 265–275, 2005.

[7] F. Cherblanc, J. Berthonneau, P. Bromblet, and V. Huon, "Influence of water content on the mechanical behaviour of limestone: role of the clay minerals content," *Rock Mechanics and Rock Engineering*, vol. 49, no. 6, pp. 2033–2042, 2016.

[8] Y. Zhao, C. Wang, L. Ning, H. Zhao, and J. Bi, "Pore and fracture development in coal under stress conditions based on nuclear magnetic resonance and fractal theory," *Fuel*, vol. 309, article 122112, 2022.

[9] T. Xiao, M. Huang, and M. Gao, "Triaxial permeability experimental study on deformation and failure processes of single-fractured rock specimens," *Shock and Vibration*, vol. 2020, 12 pages, 2020.

[10] L. Xie, P. Jin, T. C. Su, X. Li, and Z. Liang, "Numerical simulation of uniaxial compression tests on layered rock specimens using the discrete element method," *Computational Particle Mechanics*, vol. 7, no. 4, pp. 753–762, 2020.

[11] Y. Zhao, J. Bi, C. Wang, and P. Liu, "Effect of unloading rate on the mechanical behavior and fracture characteristics of sandstones under complex triaxial stress conditions," *Rock Mechanics and Rock Engineering*, vol. 54, no. 9, pp. 4851–4866, 2021.

[12] L. Ding and Y. Liu, "Study on the fractal model of erosion of soft rock by water immersed: case study erosion of metamorphic slate," *Geotechnical and Geological Engineering*, vol. 39, no. 7, pp. 5183–5189, 2021.

[13] S. Cowie and G. Walton, "The effect of mineralogical parameters on the mechanical properties of granitic rocks," *Engineering Geology*, vol. 240, pp. 204–225, 2018.

[14] Y. Zhao, C. Wang, M. Teng, and J. Bi, "Observation on microstructure and shear behavior of mortar due to thermal shock," *Cement and Concrete Composites*, vol. 121, article 104106, 2021.

[15] T. Xiao, M. Huang, C. Cheng, and Y. He, "Experimental investigation on the mechanical characteristics and deformation behaviour of fractured rock-like material with one single fissure under the conventional triaxial compression," *Shock and Vibration*, vol. 2018, Article ID 2608639, 11 pages, 2018.

[16] Z. Liu, C. Y. Zhou, B. T. Li, Y. Q. Lu, and X. Yang, "A dissolution-diffusion sliding model for soft rock grains with hydro-mechanical effect," *Journal of Rock Mechanics and Geotechnical Engineering*, vol. 10, no. 3, pp. 457–467, 2018.

[17] Y. Zhao, Y. Zhang, H. Yang, Q. Liu, and G. Tian, "Experimental study on relationship between fracture propagation and pumping parameters under constant pressure injection conditions," *Fuel*, vol. 307, article 121789, 2022.

[18] Z. Y. Chai, T. H. Kang, and G. R. Feng, "Effect of aqueous solution chemistry on the swelling of clayey rock," *Applied Clay Science*, vol. 93-94, pp. 12–16, 2014.

[19] H. P. Yuan, P. Cao, and W. Z. Xu, "Mechanism study on subcritical crack growth of flabby and intricate ore rock," *Transactions of Nonferrous Metals Society of China*, vol. 16, no. 3, pp. 723–727, 2006.

[20] W. Yuan, X. Liu, and Y. Fu, "Study on deterioration of strength parameters of sandstone under the action of dry-wet cycles in acid and alkaline environment," *Arabian Journal for Science and Engineering*, vol. 43, no. 1, pp. 335–348, 2018.

[21] Z. Qin, H. Fu, and X. Chen, "A study on altered granite mesodamage mechanisms due to water invasion-water loss cycles," *Environmental Earth Sciences*, vol. 78, no. 14, pp. 1–10, 2019.

[22] P. Guo, D. Ren, and Y. Xue, "Simulation of multi-period tectonic stress fields and distribution prediction of tectonic fractures in tight gas reservoirs: a case study of the Tianhuan Depression in western Ordos Basin, China," *Marine and Petroleum Geology*, vol. 109, pp. 530–546, 2019.

[23] T. Jiang, X. Pan, J. Lei, J. Zhang, and W. Wang, "Rupture and crack propagation in artificial soft rock with preexisting fractures under uniaxial compression," *Geotechnical and Geological Engineering*, vol. 37, no. 3, pp. 1943–1956, 2019.

[24] Y. Zhao, C. L. Wang, and J. Bi, "Analysis of fractured rock permeability evolution under unloading conditions by the model of elastoplastic contact between rough surfaces," *Rock Mechanics and Rock Engineering*, vol. 53, no. 12, pp. 5795–5808, 2020.

[25] Y. Zhang, L. N. Y. Wong, and K. K. Chan, "An extended grain-based model accounting for microstructures in rock deformation," *Journal of Geophysical Research: Solid Earth*, vol. 124, no. 1, pp. 125–148, 2019.

[26] X. Liu, D. Q. Li, Z. J. Cao, and Y. Wang, "Adaptive Monte Carlo simulation method for system reliability analysis of slope stability based on limit equilibrium methods," *Engineering Geology*, vol. 264, article 105384, 2020.

[27] M. A. Coombes and L. A. Naylor, "Rock warming and drying under simulated intertidal conditions, part II: weathering and biological influences on evaporative cooling and near-surface micro-climatic conditions as an example of biogeomorphic ecosystem engineering," *Earth Surface Processes and Landforms*, vol. 37, no. 1, pp. 100–118, 2012.

[28] X. Liu, M. Jin, D. Li, and L. Zhang, "Strength deterioration of a shaly sandstone under dry–wet cycles: a case study from the Three Gorges Reservoir in China," *Bulletin of Engineering Geology and the Environment*, vol. 77, no. 4, pp. 1607–1621, 2018.

[29] J. A. Pineda, E. Romero, M. De Gracia, and D. Sheng, "Shear strength degradation in claystones due to environmental effects," *Géotechnique*, vol. 64, no. 6, pp. 493–501, 2014.

[30] W. Hua, S. Dong, Y. Li, J. Xu, and Q. Wang, "The influence of cyclic wetting and drying on the fracture toughness of sandstone," *International Journal of Rock Mechanics and Mining Sciences*, vol. 78, pp. 331–335, 2015.

[31] K. G. Li, D. P. Zheng, and W. H. Huang, "Mechanical behavior of sandstone and its neural network simulation of constitutive model considering cyclic drying-wetting effect," *Rock and Soil Mechanics*, vol. 34, no. S2, pp. 168–173, 2013.